Locked nucleic acids (LNAs) reveal sequence requirements and kinetics of Xist RNA localization to the X chromosome

Kavitha Sarma[a], Pierre Levasseur[b], Alexander Aristarkhov[b], and Jeannie T. Lee[a,1]

[a]Howard Hughes Medical Institute, Department of Molecular Biology, Massachusetts General Hospital, Department of Genetics, Harvard Medical School, Boston, MA 02114; and [b]Exiqon Corporation, Woburn, MA 01801

Edited* by Arthur D. Riggs, Beckman Research Institute of the City of Hope, Duarte, CA, and approved October 8, 2010 (received for review July 9, 2010)

A large fraction of the mammalian genome is transcribed into long noncoding RNAs. The RNAs remain largely uncharacterized as the field awaits new technologies to aid functional analysis. Here, we describe a unique use of locked nucleic acids (LNAs) for studying nuclear long noncoding RNA, an RNA subclass that has been less amenable to traditional knockdown techniques. We target LNAs at Xist RNA and show displacement from the X chromosome with fast kinetics. Xist transcript stability is not affected. By targeting different Xist regions, we identify a localization domain and show that polycomb repressive complex 2 (PRC2) is displaced together with Xist. Thus, PRC2 depends on RNA for both initial targeting to and stable association with chromatin. H3K27-trimethyl marks and gene silencing remain stable. Time-course analysis of RNA relocalization suggests that Xist and PRC2 bind to different regions of the X at the same time but do not reach saturating levels immediately. Thus, LNAs provide a tool for studying an emerging class of regulatory RNA and offer a window of opportunity to target epigenetic modifications with possible therapeutic applications.

dosage compensation | X inactivation

The mammalian genome synthesizes a large number of long noncoding RNAs (lncRNA) (1, 2), but their structure and function remain largely uncharacterized. Although siRNA/shRNA knockdown technologies have become staples in functional analysis of microRNAs (miRNAs) and cytoplasmically localized RNAs (3–5), these methods are less consistently effective for lncRNAs localized to the nucleus. Development of methods to target nuclear lncRNAs would therefore advance the field. Here we investigate the function of a lncRNA using locked nucleic acid (LNA) technology. LNAs are nucleic acid analogs in which the ribose ring is "locked" by a methylene bridge between the 2′ oxygen and the 4′ carbon. LNA bases form standard Watson–Crick base pairs but increase the rate and stability of the basepairing reaction (6). LNAs also have increased affinity to base pair with RNA as compared with DNA. These properties render LNAs especially useful as probes for fluorescence in situ hybridization and comparative genomic hybridization, as antagomirs for miRNAs, and as antisense oligonucleotides to block mRNA translation (3, 4). Below we describe another use of LNA by demonstrating its ability to displace a *cis*-acting nuclear lncRNA with fast kinetics, a property that enables study of the RNA's behavior in ways not possible before.

Xist RNA is a 17-kb ncRNA that initiates X-chromosome inactivation (XCI) as the RNA coats the inactive X (Xi) *in cis* (7–10). How Xist RNA localizes along the X is currently unclear. Genetic analyses have identified a silencing domain at the 5′ end known as "repeat A" (11), shown to directly recruit polycomb proteins to the Xi (12). The rest of the RNA is thought to localize Xist to Xi but has yet to be characterized in detail. Several other conserved repeated motifs, termed repeats B–F, have been identified in Xist (8, 9). Repeat C is located 3 kb downstream of repeat A and contains 14 tandem repeats of a C-rich sequence with ∼90% interrepeat homology. Previous work showed that treating cells for 6 d with an antisense peptide nucleic acid (PNA) against repeat C led to loss of Xist from Xi heterochromatin (13), suggesting that the repeat C region may harbor an essential element. Curiously, it has also been shown that deleting repeat C on an *Xist* transgene has no effect on XCI (11). To examine repeat C function, below we target LNAs against this region and discover their ability to displace Xist RNA and PRC2 with fast kinetics. We report unique findings regarding de novo localization of Xist RNA and PRC2 onto Xi.

Results

LNAs Targeting *Xist* Repeat C Rapidly Displace Xist RNA from Xi. We aligned repeat C using Geneious software and synthesized LNAs complementary to two regions with a high degree of interrepeat conservation (Fig. 1*A*). The first LNA showed conservation in all 14 repeats (LNA-C1) and the second in 13 of 14 (LNA-C2) (Fig. 1 *A* and *B*). LNAs were nucleofected separately into transformed mouse embryonic fibroblasts (MEFs), and the cells were fixed on slides at various times between 0 min (immediately after nucleofection) and 8 h postnucleofection. To examine effects on Xist RNA, we performed RNA fluorescence in situ hybridization (FISH) using Xist-specific probes. [MEF cells are tetraploid due to transformation; each tetraploid cell has two Xa and two Xi]. In controls transfected with scrambled LNAs (LNA-Scr), robust Xist clouds were seen in 80–90% of cells at all time points (Fig. 1 *B* and *C*). Intriguingly, introduction of either LNA-C1 or -C2 resulted in immediate loss of Xist RNA from Xi (Fig. 1 *B* and *C*; LNA-C1 shown, with similar results for LNA-C2). Even at $t = 0$, ∼10% of nuclei displayed faint and diffuse Xist RNA clusters (Fig. 1*B*, asterisk; Fig. 1*C*, yellow bars) ($n = 149$). The percentage of nuclei with full Xist clouds continued to drop during the first hour and reached a minimum at $t = 60$ min (21%, $n = 190$). These findings indicate that LNAs disrupted Xist binding to chromatin as soon as they were introduced. However, the loss of Xist from Xi was transient, as pinpoints of Xist RNA typical of nascent transcripts seen in undifferentiated embryonic stem (ES) cells, became visible at $t = 3$ h (Fig. 1*B*, arrows; Fig. 1*C*, red bars) (18%, $n = 190$ at 1 h; 36%, $n = 123$ at 3 h). Full recovery of Xist clouds was not seen until 8–24 h postnucleofection (Fig. 1*B*) (81% at 8 h, $n = 117$).

We next addressed whether LNAs had similar effects in mouse ES cells (Fig. S1*A*), which recapitulate XCI as the cells differentiate in culture. Undifferentiated wild-type female ES cells express low levels of Xist RNA, visible as pinpoint signals by RNA FISH. By day 6 of differentiation, ∼40% of cells would normally have upregulated Xist RNA (Fig. S1*B*). When ES cells were nucleofected with LNA-C1 on day 6, Xist displacement occurred rapidly, reaching a maximum at 1 h and recovering by 8 h (Fig. S1*B*). Thus, LNAs were effective in ES cells as well as in somatic cells. These results contracted sharply with those obtained from MEFs

Author contributions: K.S. and J.T.L. designed research; K.S. performed research; P.L. and A.A. contributed new reagents/analytic tools; K.S. and J.T.L. analyzed data; and K.S. and J.T.L. wrote the paper.

The authors declare no conflict of interest.

*This Direct Submission article had a prearranged editor.

[1]To whom correspondence should be addressed. E-mail: lee@molbio.mgh.harvard.edu.

This article contains supporting information online at www.pnas.org/lookup/suppl/doi:10.1073/pnas.1009785107/-/DCSupplemental.

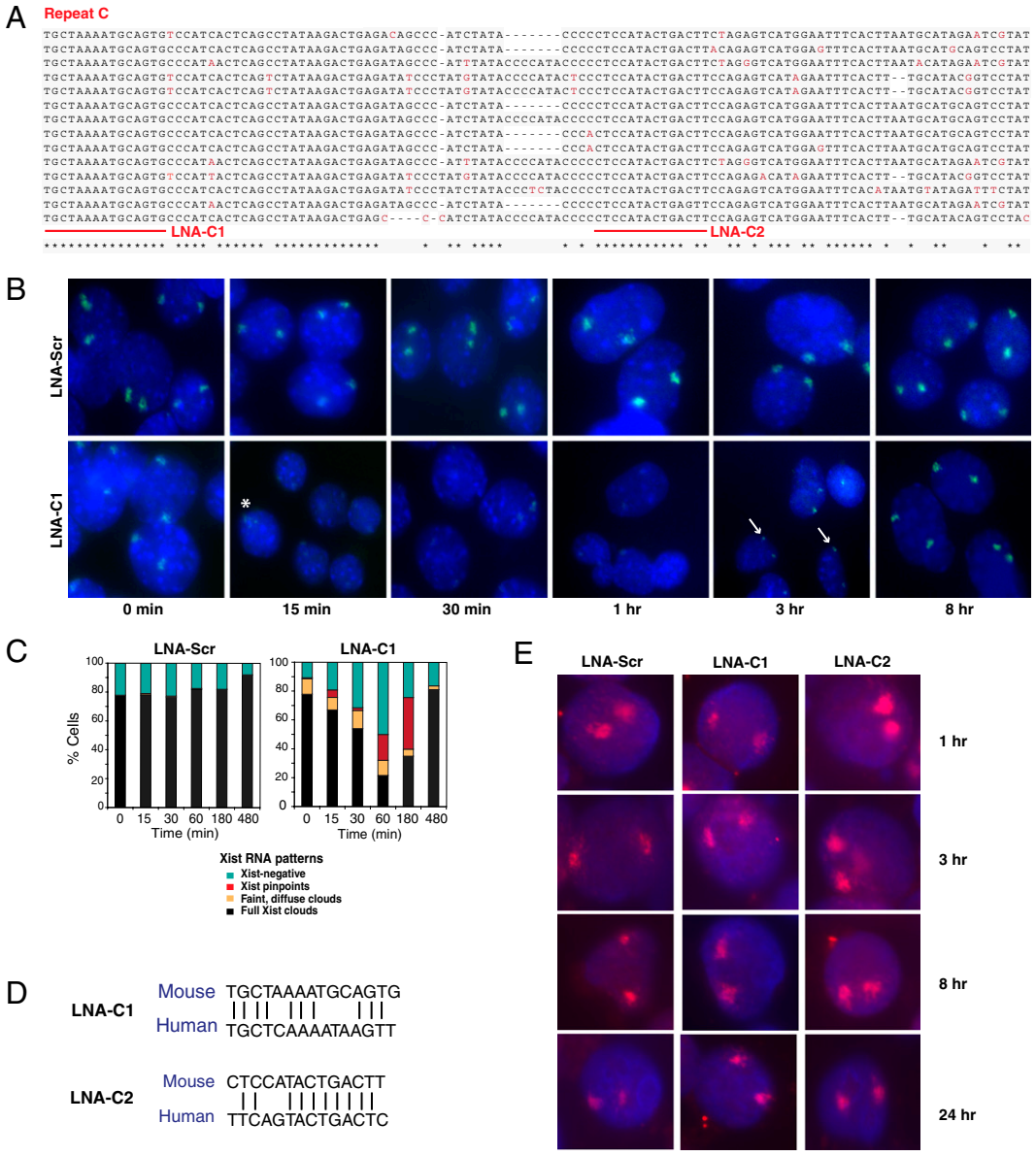

Fig. 1. LNAs targeting *Xist* repeat C abolish Xist RNA localization to Xi. (*A*) Alignment of 14 tandem mouse repeat C. Mismatches are shown in red. The regions targeted by LNAs are indicated by a red line. (*B*) Xist RNA FISH at indicated time points after LNA nucleofection. Results shown for LNA-C1, but LNA-C2 gives similar results. Xist RNA, green. Asterisk, diffuse Xist cluster; arrows, pinpoint Xist signals. (*C*) Quantitation of the results in *B*. (*D*) Alignment of mouse and human repeat C regions targeted by the LNAs (*Left*). (*E*) XIST RNA FISH performed in human 293 cells nucleofected with LNAs. XIST RNA, red.

nucleofected with siRNAs or shRNAs toward the same region of Xist. Neither siRNAs nor shRNAs led to loss of Xist at the 1-, 3-, or 24-h time points, and partial decreases in Xist clouds occurred only at 48 h (Fig. S2; 83%, $n = 84$ at 1 h; 80%, $n = 106$ at 24 h). Thus, LNAs can be used efficiently to target lncRNAs with rapid kinetics, faster than siRNAs or shRNAs, in multiple cell types.

To test the specificity of the LNAs, we nucleofected human 293 cells with the repeat C LNAs. Sequence comparison between the mouse and human Xist/XIST revealed that the region targeted by LNA-C1 is conserved in 10 of 15 nt and in 10 of 14 nt for LNA-C2 (Fig. 1*D*). Nucleofection of scrambled LNAs followed by RNA FISH in human cells showed two normal XIST clouds in nearly all cells (92%, $n = 108$) (Fig. 1*E*). Similarly, nucleofection with either LNA-C1 or LNA-C2 did not change the XIST clouds (LNA-C1, 89%, $n = 126$; LNA-C2, 85%, $n = 139$). Thus, mouse repeat C LNAs do not affect human XIST localization, suggesting that they function in a species-specific manner. To determine whether human repeat C could displace human XIST, we nucleofected LNAs complementary to the human repeat C into 293 cells, but observed no loss of XIST clouds (Fig. S3; 91%, $n = 103$ at 1 h; 87%, $n = 95$ at 3 h and 92%, $n = 85$ at 8 h). This indicates that, although repeat C may play a role in humans, additional human elements function in RNA localization. Whereas mouse repeat C occurs 14 times, the human repeat is present only once (8, 9).

Xist RNA Is Displaced Without Transcript Destabilization. Several mechanisms could explain the disappearance of Xist. LNAs could anneal to the complementary region and target Xist for degradation. Alternatively, hybridization to LNAs could displace Xist RNA from Xi without affecting transcript stability. To distinguish between these possibilities, we quantitated Xist levels relative to Gadph levels (control) by qRT-PCR at different times. At 1 h when Xist clouds were no longer visible, Xist levels remained comparable to that seen in LNA-Scr (Fig. 2*A*). Even at 3 and 8 h, Xist levels did not change significantly. These results showed that,

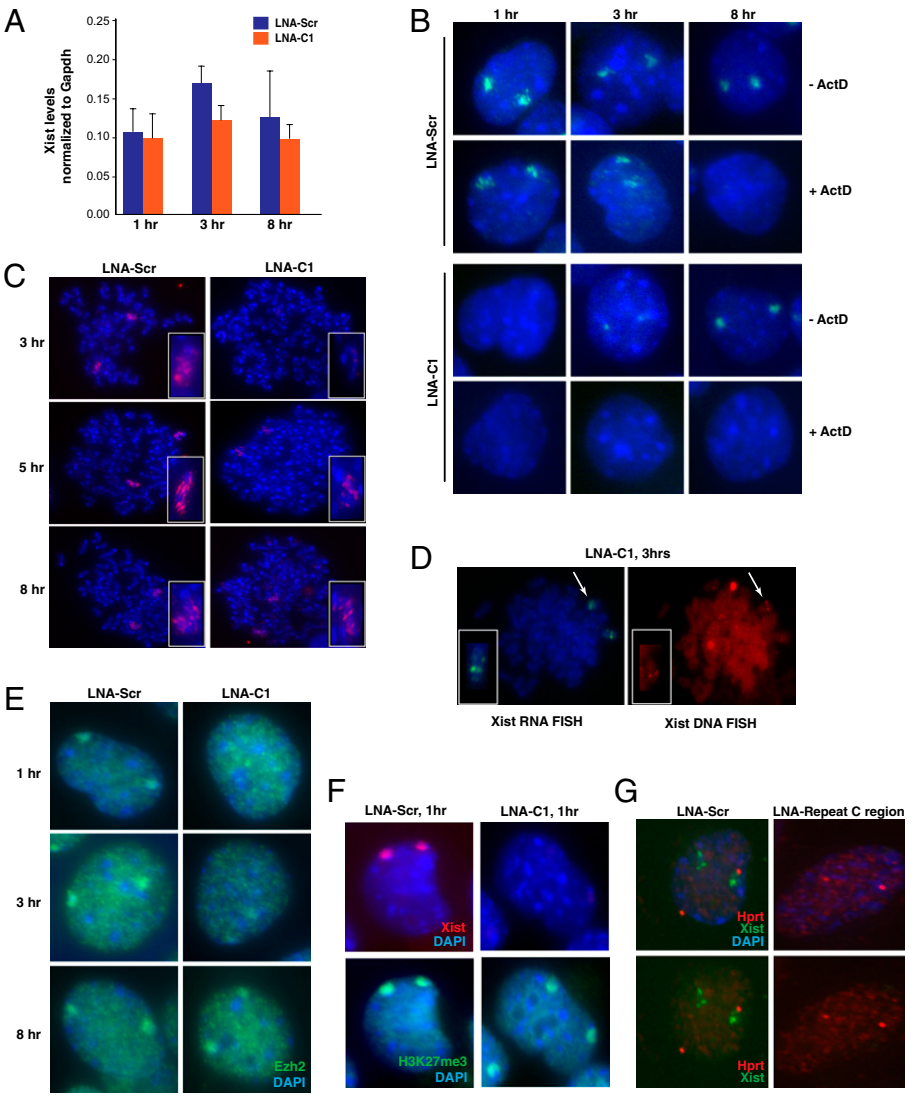

Fig. 2. Xist RNA displacement is accompanied by loss of PRC2 localization and recovery occurs initially near *Xist*. (*A*) Real-time qRT-PCR analysis of Xist levels, normalized to Gapdh RNA. (*B*) Xist RNA FISH in cells treated with or without ActD after LNA nucleofection. Xist RNA, green. (*C*) Xist RNA FISH on metaphase chromosomes after LNA nucleofection. Xist RNA, red. (*D*) Xist RNA FISH (green) followed by *Xist* DNA FISH (red) in metaphase spreads from cells at 3 h post-LNA treatment. Arrows, *Xist* locus. (*E*) Immunostaining for Ezh2 (green). (*F*) Immunostaining for H3K27me3 (green). Xist RNA FISH (red) was performed to confirm loss of Xist from Xi at 1 h. (*G*) Two-color RNA FISH detecting Hprt and Xist RNA simultaneously at 3 h after nucleofection.

LNAs function by blocking Xist interaction with chromatin rather than altering the RNA's stability.

The rapid displacement of Xist and the slow kinetics of recovery provided the opportunity to investigate several unanswered questions regarding Xist's mechanism of localization. To ask whether reappearance of Xist on Xi is due to relocalization of displaced Xist molecules or to coating by newly synthesized RNA, we performed time-course analysis in the presence of actinomycin D (ActD), an inhibitor of RNA polymerase II. Previous studies have shown that the half-life of Xist in the cell is ≈4–6 h (14–16). We reasoned that treating cells with ActD for 0–8 h would prevent new synthesis of Xist RNA during this time frame and that reappearance of Xist clouds would imply relocalization of displaced RNA back onto Xi. We introduced LNAs into cells and allowed them to recover in medium containing ActD. In LNA-Scr samples, Xist clouds were clearly visible at all time points without ActD. With ActD, Xist clouds were apparent in the 1- and 3-h time points and were lost by 8 h, consistent with a 4- to 6-h half-life (Fig. 2*B*). In LNA-C1 treated samples recovered without ActD, pinpoints of Xist were visible at 3 h and clouds were restored by the 8-h time point. However, with ActD, Xist clouds were never restored, neither fully nor partially (Fig. 2*B*). Thus, Xist recovery after LNA-mediated displacement is due to new RNA synthesis and not relocalization of the displaced transcript.

Xist RNA Localizes Near the X-Inactivation Center First. Taking further advantage of the rapid displacement and slow recovery, we asked whether Xist spreads in a piecemeal fashion or localizes simultaneously throughout Xi. One hypothesis is that coating initiates near the *Xist* locus and proceeds to both ends of the chromosome through booster elements located along the X (17). Alternatively, coating can occur all at once through multiple X-linked seeding points, which would promote local spreading. We analyzed Xist localization on metaphase chromosomes during the 3- to 8-h period of recovery. In cells treated with LNAScr, all metaphase chromosomes coated with Xist RNA showed a banded pattern as described in earlier works (18–20) (Fig. 2*C*). By contrast, LNA-C1–treated cells gave intermediate patterns. At 1 h, no metaphase chromosomes showed a coat of Xist RNA (0%, n = 41). At 3 h when Xist RNA was a pinpoint in interphase cells, the predominant pattern was a combination of a single bright band in the middle of the metaphase chromosome together with a small number of very faint bands elsewhere on the X (52%, n = 46) (Fig. 2*C*). To determine whether the strong RNA band was localized to the *Xist* region, we carried out RNA FISH on nondenatured nuclei and followed with denaturation and hybridization to an *Xist* probe. Indeed, the focal RNA band observed at the 3-h mark colocalized with the *Xist* region (Fig. 2*D*). At 5 h, intermediate degrees of coating and intensities could be seen (Fig. 2*D*, 68%, n = 38). At 8 h, the predominant pattern was the whole-chromosome painting pattern typical of control cells (78%, n =

38). In controls, intermediate patterns were not observed at any time. These findings argue that Xist RNA initially binds nearby, but seems to spread to the rest of Xi at the same time, within the temporal and spatial resolution of the FISH technique.

Xist RNA Displacement Is Accompanied by Loss of PRC2 Localization. The pattern of polycomb repressive complex 2 (PRC2) binding to Xi has been of considerable interest, as its Ezh2 subunit catalyzes trimethylation of histone H3 at lysine 27 (H3K27me3). Several studies have shown that PRC2 localizes to Xi in an Xist-dependent manner, as deleting Xist in ES cells precludes PRC2 recruitment during differentiation and conditionally deleting Xist in MEF cells results in loss of PRC2 on Xi (21–24). However, the kinetics with which PRC2 is recruited to and lost from X are not known. Because Xist RNA directly recruits PRC2 (12), we asked whether LNA-mediated displacement of Xist results in immediate loss of PRC2 by immunostaining for Ezh2 in MEFs after LNA delivery. Upon treatment with the repeat C LNAs, Ezh2 was rapidly lost (Fig. 2*E*). There was nearly perfect concordance between Xist and PRC2 loss. At 1 and 3 h, Ezh2 foci were never observed in nuclei that had lost Xist and, conversely, were always observed in nuclei with restored Xist clouds. The loss of Ezh2 on Xi was not due to Ezh2 protein turnover (Fig. 3*E*). Transient displacement of PRC2, however, does not lead to appreciable H3K27me3 loss within the 1- to 8-h time frame (Fig. 2*F*). Thus, PRC2's localization onto Xi depends on Xist RNA for both initial targeting and for stable association after XCI is established, but the H3K27me3 mark is stable in the short term when Xist and PRC2 are displaced.

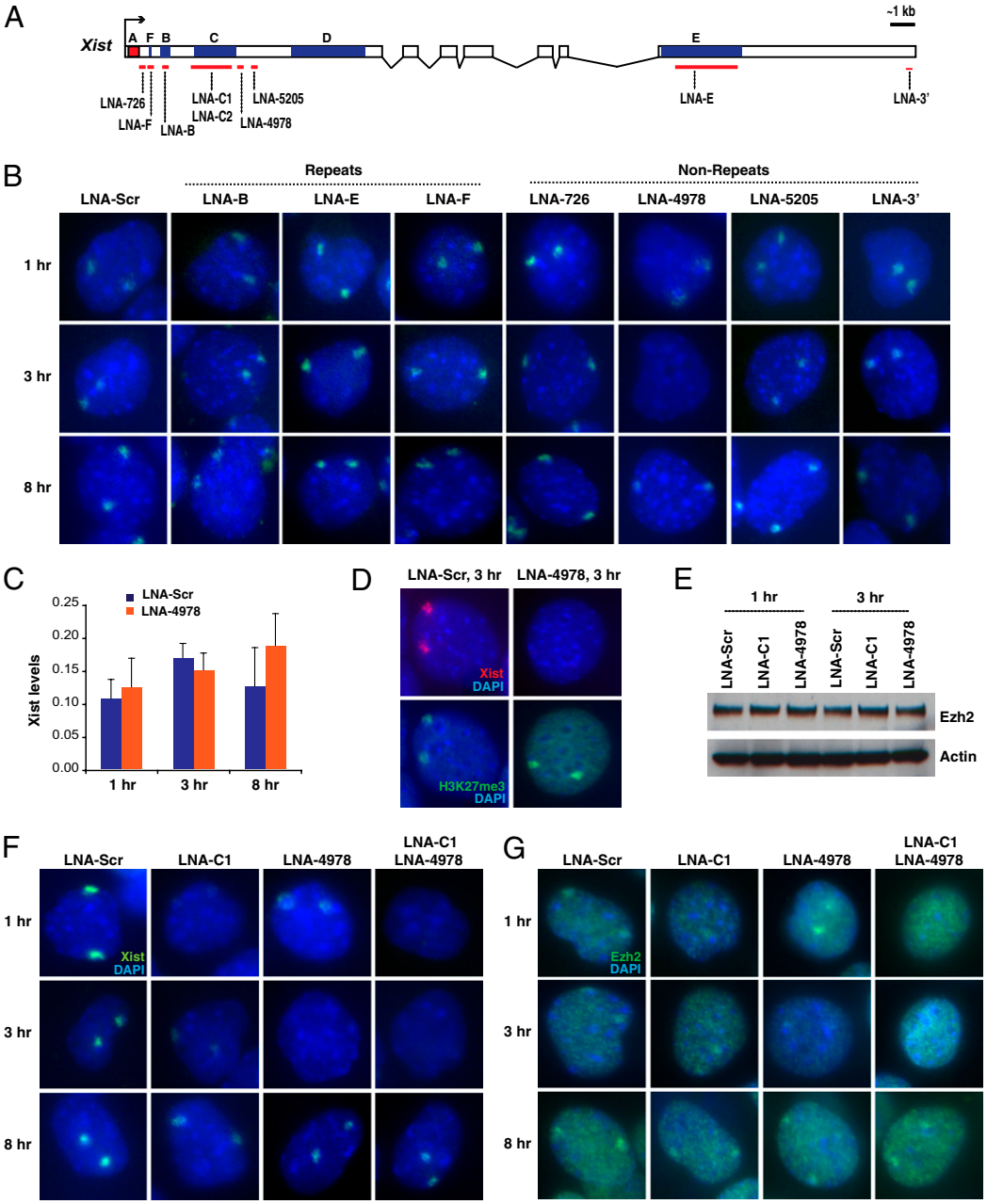

Fig. 3. A broader domain around repeat C is required for Xist localization. (*A*) Map of *Xist* exon/intron structure and locations of LNAs used. (*B*) Time-course Xist RNA FISH analysis in cells treated with indicated LNAs. Xist, green. (*C*) qRT-PCR of Xist levels, normalized to Gapdh quantities. (*D*) Immunostaining for H3K27me3 (green) and RNA FISH for Xist (red). (*E*) Western blot with Ezh2 antibodies. Actin is used as a loading control. (*F*) Xist RNA FISH (green) after nucleofection with indicated LNAs. (*G*) Ezh2 immunostaining after nucleofection with indicated LNAs.

Given this, we asked whether LNAs affected gene silencing. At 3 h when Xist was maximally displaced, we performed RNA FISH for Xist and either Pgk1 or Hprt, two X-linked genes subject to XCI. In control (LNA-Scr) cells, we observed Xist clouds from Xi and nascent Pgk1 or Hprt transcripts from Xa (Fig. 2*G* and Fig. S4). Nucleofection with LNA-C1 and LNA-4978 did not change the expression pattern, as two foci of Pgk1 transcripts were still seen in 79% (n = 39) of controls and 80% (n = 36) of LNA–treated cells, and two foci of Hprt RNA were seen in 84% (n = 44) of controls and 79% (n = 35) of LNA–treated cells. Four foci of Pgk1 or Hprt transcripts were never seen. Thus, consistent with retention of H3K27me3, silencing was not disrupted by transient loss of Xist and PRC2.

Broader Domain Around Repeat C Is Required for Xist Localization. We next investigated other conserved repeats within Xist. As repeat A has already been shown to be essential for targeting PRC2, we focused on repeats B, E, and F, and found that Xist localization was not affected by targeting any repeat individually or in combination (Fig. 3*A* and *B*). We also tested conserved unique regions of Xist, including LNA-726 (between repeats A and F), LNA-4978, and LNA-5205 (between repeats C and D), and LNA-3′ (distal terminus of Xist) (Fig. 3*A*). None affected Xist localization except for LNA-4978, which corresponds to a 15-nt element located 280 bp downstream of repeat C (Fig. 3*B*). LNA-4978 induced effects similar to LNA-C1/C2 but differed by its slower kinetics. At 1 h, Xist clouds were still visible but appeared faint and dispersed (78%, n = 125). The number of clouds reached a minimum at 3 h (25%, n = 158). At 8 h, Xist was visible as small pinpoints (Fig. 3*B*; 39%, n = 123). Recovery was not complete until the 24-h time point. As for repeat C LNAs, loss of Xist was not due to RNA turnover, as determined by qRT-PCR (Fig. 3*C*), and Ezh2 was displaced without affecting H3K27me3 (Fig. 3*D*) or change in Ezh2 protein level (Fig. 3*E*). Therefore, Xist localization to chromatin involves a broader region encompassing both repeat C and a unique region directly downstream of the repeat.

To determine whether the two motifs cooperate, we nucleofected LNA-4978 and LNA-C1 separately or together into MEFs (Fig. 3 *F* and *G*). As expected, treating with LNA-C1 alone resulted in loss of Xist RNA clouds by 1 h and recovery beginning at 3 h, and treating with LNA-4978 showed loss and recovery at 3 h and 8 h, respectively. Treating with both LNAs expanded the window of Xist depletion: We observed loss of Xist RNA and Ezh2 by 1 h (as was the case for LNA-C1 alone) and recovery did not begin until 8 h (as was the case for LNA-4978 alone). Thus, the LNA effects were additive, not synergistic, as the effects were not enhanced beyond the widening of the Xist-depleted time window.

Ezh2 Recovery After LNA Nucleofection Is Slow but Uniform Along Xi. Finally, we asked whether Ezh2 retargeting to Xi closely follows the piecemeal relocalization of Xist RNA during the recovery phase. Because PRC2 generally binds near promoters (25, 26), we analyzed Ezh2 localization at X-gene promoters by quantitative chromatin immunoprecipitation (qChIP) (Fig. 4*A*). Although female cells have two Xs and Ezh2 epitopes pulled down by the antibody could theoretically come from either Xa or Xi, evidence indicates that the bulk of Ezh2 and H3K27me3 is bound to Xi (21–24). We observed that Ezh2 was indeed enriched at promoters of genes that are silenced on Xi (e.g., *Xmr* and *Pgk1*), but not at promoters of genes (e.g., *Jarid1c*) that escape XCI (Fig. 4*B*). We then nucleofected MEF cells with LNA-C1 and performed qChIP using anti-Ezh2 antibodies between 1 and 24 h. At t = 1 h, Ezh2 levels decreased at all tested gene promoters to background levels (Fig. 4*C*), indicating that depletion of promoter-bound Ezh2 closely followed Xist displacement along Xi. At the 3- and 8-h points, there was a gradual, uniform increase in Ezh2 levels across all genes, with many genes appearing to have reached saturating amounts of Ezh2 by t = 8 h. On promoters with the highest levels of Ezh2 at t = 0 h (Fig. 4*B*), Ezh2 levels did not fully recover until 24 h (Fig. 4*C*). In contrast, Ezh2 levels at the *En1* control, a known autosomal PRC2 target (27), did not change significantly (Fig. 4*D*). We conclude that Ezh2 levels fall and rise with similar kinetics throughout Xi. The loss of Xist RNA and Ezh2 binding between 1 and 8 h presents a window of opportunity during which cells could be reprogrammed to achieve novel epigenetic states.

Discussion

Using LNAs, our study has followed the kinetics of Xist and PRC2 localization along Xi. Repeat C region is essential for RNA binding to chromatin. Targeting this region with LNAs rapidly disrupts RNA–chromatin interaction and leads to displacement of Xist RNA without affecting RNA stability. PRC2 is immediately

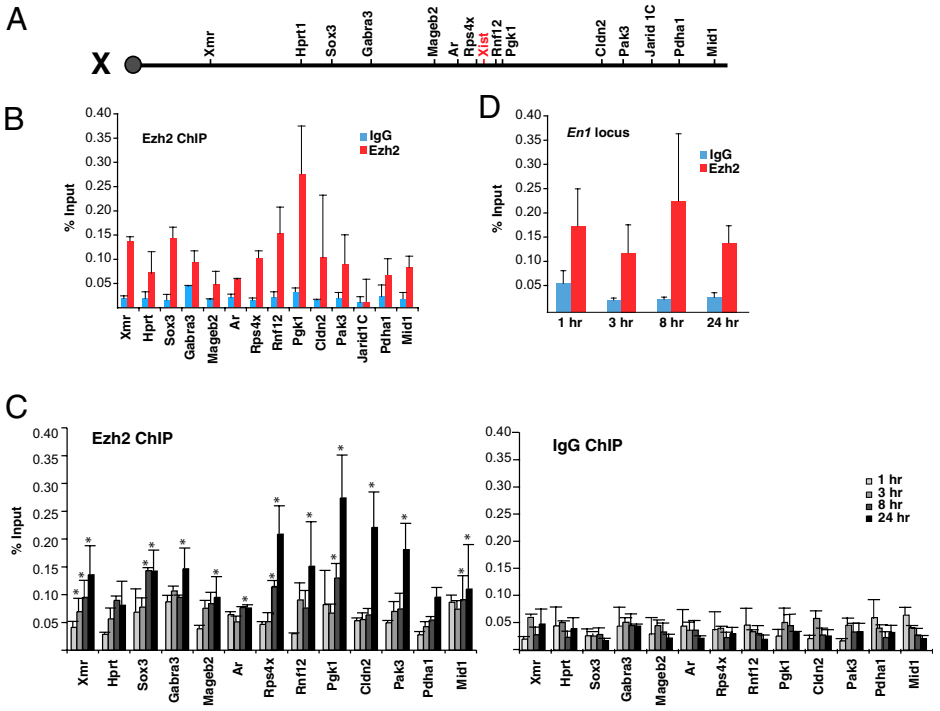

Fig. 4. Ezh2 recovery after LNA nucleofection is uniform along Xi but slow in kinetics. (*A*) Schematic representation of X genes. (*B*) Ezh2 ChIP analysis at X genes. (*C*) ChIP analysis of Ezh2 after LNA nucleofection. *P < 0.05 by the Student's t test. (*D*) ChIP analysis of Ezh2 enrichment on the autosomal *En1* promoter.

lost from Xi, demonstrating that RNA is required not only to target PRC2 initially but also to maintain a stable association with Xi. From a commercial and clinical perspective, the time points between 1 and 8 h potentially define a window for epigenetic reprogramming. We envision that, by targeting nuclear lncRNAs, LNAs or similar polymers might be used to manipulate the chromatin state of cells in culture or in vivo, by transiently eliminating the regulatory RNA and associated proteins long enough to alter the underlying locus for therapeutic purposes.

It is remarkable that targeting a small region within a 17-kb RNA can produce such dramatic effects. The rapid effects suggest that the Xist RNA–protein complex may be anchored to Xi chromatin via repeat C. Alternatively, the LNA's binding to repeat C could change RNA conformation and interfere with a remote anchoring domain. Whereas RNA displacement occurs with rapidly, the recovery period is prolonged. Although full Xist clouds are restored within 8 h, the full complement of PRC2 is not recovered for up to 24 h. This implies that, during the spread of XCI, synthesis of the RNA is not the rate-limiting step; rather, it is the recruitment of associated silencing proteins such as PRC2. The rapid loss of Xist and the slow kinetics of recovery provided a time frame to investigate Xist's spreading pattern relative to that of PRC2. Time-course analysis during the recovery phase indicates that Xist RNA binds most strongly near the *Xist* locus at first but spreads to the rest of Xi at the same time. Similarly, PRC2 is recruited synchronously throughout the X. Interestingly, neither Xist nor PRC2 levels reach saturation immediately, as the coating of Xist is not complete until 8 h and binding of PRC2 does not peak until 24 h. Combined, this analysis implies that establishment of chromosomewide silencing may be relatively slow.

In summary, we have demonstrated that LNAs can be used as a valuable tool to aid analysis of lncRNAs. Advantages offered by an LNA-based system are the relatively low costs, easy delivery, and rapid action. Additionally, LNAs make possible the systematic targeting of domains within much longer nuclear transcripts. Although a PNA-based system has been described earlier, the effects on Xi were apparent only after 6 d (13). The LNA technology therefore brings us a step closer to high-throughput screens for functional analysis of lncRNAs and also provides a unique tool to manipulate chromatin states in vivo for therapeutic applications.

Materials and Methods

LNA Nucleofection. A total of 2×10^6 SV40T transformed MEFs were resuspended in 100 μL of Mef nucleofector solution (Lonza). Cy3-labeled LNAs were added to a final concentration of 2 μM. The cells were transfected using the T-20 program. A total of 2 mL of culture medium was added to the cells and 100 μL of this suspension was plated on one gelatinized 10-well slide per time point. LNA sequences were designed using Exiqon software (www.exiqon.com). Modified LNA bases were strategically introduced to maximize target affinity (Tm) while minimizing self-hybridization score. The LNA sequences (from 5′ to 3′) were as follows: LNA-Scr, GTGTAACACGTCTATACGCCCA; LNA-C1, CACTGCATTTTAGCA; LNA-C2, AAGTCAGTATGGAG; LNA-B, AGGGGCTGGGGCTGG; LNA-E, ATAGACACACAAAGCA; LNA-F, AAAGCCCGCCAA; LNA-4978, GCTAAATGCACACAGGG; LNA-5205,CAGTGCAGAGGTTTTT LNA-726, TGCAATAACTCACAAAACCA; and LNA-3′, ACCCACCCATCCACCCACCC.

Real-Time PCR. Total RNA was extracted after nucleofection using TRIzol (Invitrogen). Reverse transcriptase reaction was performed using the SuperScript II kit and real-time PCR performed on cDNA samples using icycler SYBR green chemistry (Biorad).

ChIP. ChIP was performed as described earlier (28) and quantitated by qPCR.

Antibodies. The antibodies for various epitopes were purchased as follows: H3K27me3, Active Motif 39535. Ezh2, Active Motif 39639 and BD Pharmingen 612666. For immunostaining, H3K27me3 antibodies were used at 1:100 dilution and Ezh2 antibodies (BD Pharmingen) at 1:500. Alexa Fluor secondary antibodies were from Invitrogen. For Western blots, Ezh2 antibodies (BD Pharmingen) were used at 1:2,000 dilution. Actin antibody (Sigma A2066) was used at 1:5,000 dilution.

DNA FISH, RNA FISH, and Immunostaining. Cells were grown on gelatinized glass slides or cytospun. RNA FISH, DNA FISH, serial RNA-DNA FISH, immunostaining, and immunoFISH were performed as described (24). Xist RNA FISH was performed using nick-translated pSx9-3 probe or an Xist riboprobe mixture. pSx9-3 was used as probe for *Xist* DNA FISH. For metaphase spreads, colchicine was added to cells for 1 h. Cells were trypsinized and resuspended in 3 mL of 0.056M KCl for 30 min at room temperature, centrifuged, and resuspended in methanol:acetic acid (3:1) fixative. After several changes of fixative, cells were dropped on a chilled slide and processed for RNA or DNA FISH.

ACKNOWLEDGMENTS. We are grateful to Y. Jeon (Howard Hughes Medical Institute, Massachusetts General Hospital, Boston) for contributing the MEF line prior to publication. We also thank Y. Jeon, D. Lessing, S. Pinter, S. Sun, and B. del Rosario for critical reading of the manuscript and all laboratory members for inspiring discussions. This work was supported by National Institutes of Health Grants F32-GM090765 (to K.S.) and RO1-GM090278 (to J.T.L.). J.T.L. is an Investigator of the Howard Hughes Medical Institute.

1. Kapranov P, Willingham AT, Gingeras TR (2007) Genome-wide transcription and the implications for genomic organization. *Nat Rev Genet* 8:413–423.
2. Mercer TR, Dinger ME, Mattick JS (2009) Long non-coding RNAs: Insights into functions. *Nat Rev Genet* 10:155–159.
3. Krützfeldt J, et al. (2005) Silencing of microRNAs in vivo with 'antagomirs.'. *Nature* 438:685–689.
4. Ørom UA, Kauppinen S, Lund AH (2006) LNA-modified oligonucleotides mediate specific inhibition of microRNA function. *Gene* 372:137–141.
5. Morris KV (2008) RNA-mediated transcriptional gene silencing in human cells. *Curr Top Microbiol Immunol* 320:211–224.
6. Petersen M, Wengel J (2003) LNA: A versatile tool for therapeutics and genomics. *Trends Biotechnol* 21:74–81.
7. Penny GD, Kay GF, Sheardown SA, Rastan S, Brockdorff N (1996) Requirement for Xist in X chromosome inactivation. *Nature* 379:131–137.
8. Brockdorff N, et al. (1992) The product of the mouse Xist gene is a 15 kb inactive X-specific transcript containing no conserved ORF and located in the nucleus. *Cell* 71:515–526.
9. Brown CJ, et al. (1992) The human XIST gene: Analysis of a 17 kb inactive X-specific RNA that contains conserved repeats and is highly localized within the nucleus. *Cell* 71:527–542.
10. Clemson CM, McNeil JA, Willard HF, Lawrence JB (1996) XIST RNA paints the inactive X chromosome at interphase: Evidence for a novel RNA involved in nuclear/chromosome structure. *J Cell Biol* 132:259–275.
11. Wutz A, Rasmussen TP, Jaenisch R (2002) Chromosomal silencing and localization are mediated by different domains of Xist RNA. *Nat Genet* 30:167–174.
12. Zhao J, Sun BK, Erwin JA, Song JJ, Lee JT (2008) Polycomb proteins targeted by a short repeat RNA to the mouse X chromosome. *Science* 322:750–756.
13. Beletskii A, Hong YK, Pehrson J, Egholm M, Strauss WM (2001) PNA interference mapping demonstrates functional domains in the noncoding RNA Xist. *Proc Natl Acad Sci USA* 98:9215–9220.
14. Sheardown SA, et al. (1997) Stabilization of Xist RNA mediates initiation of X chromosome inactivation. *Cell* 91:99–107.
15. Sun BK, Deaton AM, Lee JT (2006) A transient heterochromatic state in Xist preempts X inactivation choice without RNA stabilization. *Mol Cell* 21:617–628.
16. Panning B, Dausman J, Jaenisch R (1997) X chromosome inactivation is mediated by Xist RNA stabilization. *Cell* 90:907–916.
17. Gartler SM, Riggs AD (1983) Mammalian X-chromosome inactivation. *Annu Rev Genet* 17:155–190.
18. Duthie SM, et al. (1999) Xist RNA exhibits a banded localization on the inactive X chromosome and is excluded from autosomal material in cis. *Hum Mol Genet* 8:195–204.
19. Chadwick BP, Willard HF (2004) Multiple spatially distinct types of facultative heterochromatin on the human inactive X chromosome. *Proc Natl Acad Sci USA* 101:17450–17455.
20. Clemson CM, Hall LL, Byron M, McNeil J, Lawrence JB (2006) The X chromosome is organized into a gene-rich outer rim and an internal core containing silenced nongenic sequences. *Proc Natl Acad Sci USA* 103:7688–7693.
21. Plath K, et al. (2003) Role of histone H3 lysine 27 methylation in X inactivation. *Science* 300:131–135.
22. Kohlmaier A, et al. (2004) A chromosomal memory triggered by Xist regulates histone methylation in X inactivation. *PLoS Biol* 2:E171.
23. Silva J, et al. (2003) Establishment of histone h3 methylation on the inactive X chromosome requires transient recruitment of Eed-Enx1 polycomb group complexes. *Dev Cell* 4:481–495.
24. Zhang LF, Huynh KD, Lee JT (2007) Perinucleolar targeting of the inactive X during S phase: Evidence for a role in the maintenance of silencing. *Cell* 129:693–706.
25. Boyer LA, et al. (2006) Polycomb complexes repress developmental regulators in murine embryonic stem cells. *Nature* 441:349–353.
26. Ku M, et al. (2008) Genomewide analysis of PRC1 and PRC2 occupancy identifies two classes of bivalent domains. *PLoS Genet* 4:e1000242.
27. Bracken AP, Dietrich N, Pasini D, Hansen KH, Helin K (2006) Genome-wide mapping of Polycomb target genes unravels their roles in cell fate transitions. *Genes Dev* 20:1123–1136.
28. Blais A, et al. (2005) An initial blueprint for myogenic differentiation. *Genes Dev* 19:553–569.